Bonding Process

2

In this chapter, the details of the wire bonding process are discussed. The bonding wire configurations used in the electronics industry are listed, and wire parameters such as wire processing, wire purity, and wire diameter are explained. Since the use of bare copper wires is a concern owing to the propensity of copper to oxidize, oxidation prevention technology is needed. The chapter discusses the two oxidation prevention technologies used in the industry, including cover gas and oxidation prevention coating. The wire bonding parameters govern the quality of formed free air balls (FABs) and subsequent first and second bonds. The effect of electrical flame-off current and firing time on formed FABs, and the effect of ultrasonic energy, bonding force, bonding temperature, and time on wire bond quality, is explained, and the optimal parameter ranges are listed. The bonding tools for copper wire bonding are explained and the failures resulting from improper bonding are also listed.

2.1 Bond Wire

Wire purity and the processing undergone by the wire during wire drawing operation determine the mechanical properties of the bonding wire. The mechanical properties relevant for wire bonding are elongation percentage and the breaking strength. Additionally, the stress state of the wire—residual stress or stress free (fully annealed)—determines the looping characteristics of the wire. The use of annealed wire reduces the variation in the bond strength and makes the bonding process less sensitive to thermal effects. A high-purity wire is desired, which is melted in a high vacuum to obtain a homogeneous microstructure. The resulting cast bar is subjected to multiple stages of drawing through a series of dies to reduce the wire diameter for bonding. The thinner the wire requirement, the more stages of wire drawing the wire undergoes. Wire processing should ensure that the wire has a clean surface and smooth finish so that it easily comes out of the spool without

P.S. Chauhan et al., *Copper Wire Bonding*, DOI 10.1007/978-1-4614-5761-9_2,

snagging [5]. Bare Cu wires of varying purity (3–6 N) are used in the industry, and the wire cost is directly proportional to the wire purity. Also, as the wire purity increases, the wire becomes softer.[1]

Bond wire manufacturers often dope pure Cu wire with additives to enhance the wire bondability and minimize the Al splash. For the same wire thickness, a Cu FAB is larger in diameter than the corresponding Au wire. Hence, to achieve the same FAB diameter, Cu wires are 2.54 μm thinner than Au wire. Bare Cu wires used in the industry have purities of 3–6 N, with 4 N as the most commonly used [42, 43]. Srikanth et al. [44] investigated Cu wires of varying purity, including 3, 4, and 5 N, and 50 μm thickness. They reported that higher purity wires have lower flow stress than lower purity wires (95.5 MPa for 5 N, 115 MPa for 4 N, and 120 MPa for 3 N), since they have fewer grains. Cu wire of 3 N purity had fine columnar grains in the initial state, as well as after melting (FAB formation). On the other hand, wires of 4 and 5 N purity had large grain sizes and few columnar grains in both the initial state and after melting. The grain direction on the FAB affects the hardness and elastic modulus of the FAB, wherein the lack of directionality results in softer wires. The low flow stress in 5 N wires was attributed to the lack of directionality in the grains. Because of the lower flow stress, a lower bonding force is required, which results in a lower Al splash. The high-purity wires showed high twinning features, which can impair the deformation processes during the bonding operation. On the other hand, for 3 and 4 N FABs, the number of grains in the [100] direction was larger than that in the [110] and [111] directions [44]. The thermomechanical processing that the wire undergoes determines the residual stress states in the wire and the mechanical properties, including the hardness and tensile strength. The grain structure of the wire can be optimized for the individual purity level by the wire processing steps, including the deformation and annealing steps during wire drawing. Optimization of wire purity and microstructure can help achieve the desired mechanical properties, such as wire elongation and tensile strength. Wires with a high elongation strength have smaller grains and higher tensile strength [45].

Another consideration for the bonding wire is the wire diameter. The choice of wire diameter depends on the compatibility with the process and the required current carrying capacity. For consumer electronics, the common wire diameter range is 18–25 μm, whereas for the power electronics, the common wire diameter range is 20–50 μm [46].

The use of bare Cu is a concern due to the propensity of Cu to readily oxidize. The use of oxidation-resistant coatings is one way to address the problem of Cu oxidation. Al-coated Cu wires for room-temperature wedge–wedge bonding have been shown to suppress oxidation and have better pull strength, better metallic contact formation, and better storage capabilities than bare Cu wires [47]. Al-coated wire is suited for room-temperature bonding on low-temperature co-fired ceramics

[1] The material purity in % or Nines scale is denoted in terms of purity in parts-per-million (ppm). For example, 1 N = 90 %, 2 N = 99 %, 3 N = 99.9 % and so on.

Table 2.1 Bonding wire comparison: Au, Cu, and PdCu [54]

	Au	Cu	PdCu
Cost	High	Low	Low (higher than Cu)
Cover gas	No need	Forming gas	Forming gas or N_2
FAB hardness	Compatible to Al	~40 % harder than Au	~10 % harder than Cu
First bond process	Good process window	Narrower than Au	Same or slightly narrower than Cu
Second bond process	Same	Same	Same
Portability requirement	Moderate	High	High
Reliability	Good	Good; more stringent mold compound than that for Au	Same or slightly better than Cu

with silver and gold metallization. Among the oxidation prevention coatings (Au, Ag, Pd, and Ni), Pd coating on Cu has shown sufficient potential to replace Au wire due to its excellent bondability and reliability at a relatively low cost [48–53]. Pd is a semi-noble metal with similarities to both Ag and Pt. PdCu is oxidation free, and Pd has good adhesion to Cu wire and higher tensile strength than bare Cu wire when bonded on Al pads. Table 2.1 shows a comparison of Au, Cu, and PdCu wires.

Because of the Pd layer on Cu wire, there is always a layer of Pd or a Pd-rich phase that protects the bonded ball from an attack of corrosion. Easing the use of Pd may also ease the stringent molding compound requirement. Pd prevents the formation of CuO and can form a bond with N_2 without requiring forming gas. Figure (2.1a, b) shows a comparison of Cu and PdCu wires bonded on Al. This comparison of the first bonds of PdCu and Cu wires shows that PdCu-bonded ball has lower Al pad splash than Cu-bonded ball.

Robustness in the second bond is the most important reason to adopt PdCu wires [52, 55]. This robustness has led to an improved C_{pk} (process capability index). The stitch pull strength of PdCu wire is more than 50 % higher than bare Cu [51]. PdCu wire on an aluminum bond pad has also been demonstrated to perform better than bare Cu in high-humidity conditions, such as in the highly accelerated stress test (HAST), pressure cooker test (PCT) [50], temperature cycling test (TCT), and high-temperature storage (HTS) test. Table 2.2 shows a bond strength and defective second bond ratio comparison of Au, Cu, and PdCu wires. The PdCu wires have a higher second bond strength than bare Cu wires and zero defective second bonds [48]. PdCu also works better at higher ultrasonic generator (USG) current levels than Cu wire. It should be noted, however, that due to the higher hardness and rigidity of PdCu over Cu, a higher bonding force is needed for PdCu wires, which could increase the risk of Al splash and pad damage [56]. Hence, careful optimization of bonding parameters is needed for PdCu wires.

Since PdCu wire has a larger diameter than bare Cu wire, the FAB diameter for PdCu wire needs to be smaller than for bare Cu wire. Because of the Pd layer on the Cu wire there is always a layer of Pd or a Pd-rich phase that protects the bonded ball from an attack of corrosion. Easing the use of Pd may also ease the stringent molding compound requirement. Pd prevents the formation of CuO and can form

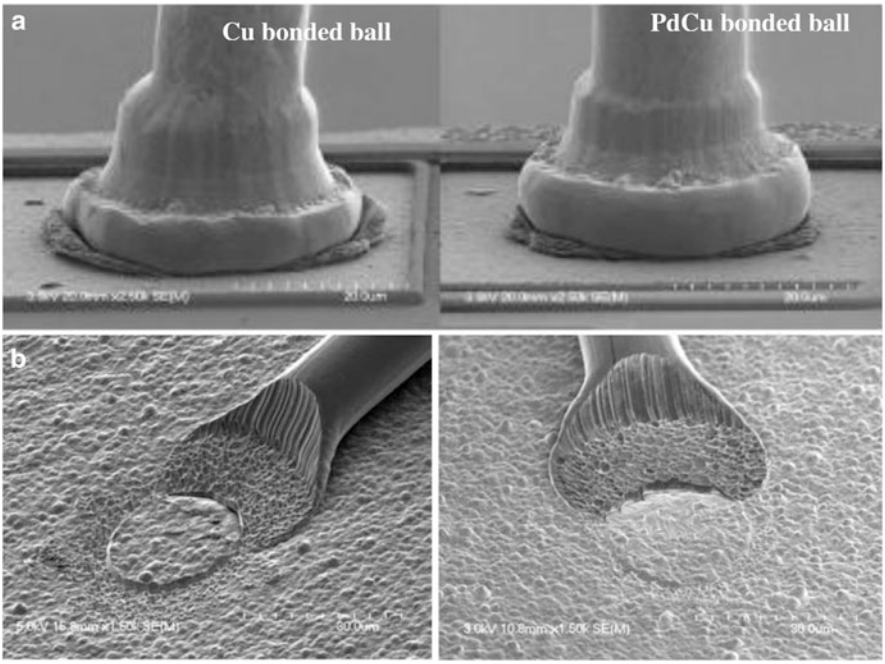

Fig. 2.1 Cu and PdCu wires: Comparison of (**a**) first and (**b**) second bonds in [51]

Table 2.2 Bond strength and defective second bond ratio comparison [48]

	Au	Cu	PdCu
First bond strength (N)	0.256	0.215	0.352
Second bond strength (N)	0.053	0.026	0.074
Defective second bond ratio (ppm)	0	7933	0

a bond with N_2 without requiring forming gas. A comparison of N_2 and forming gas for PdCu wire (15 μm) showed that forming gas is superior to N_2 since it is not sensitive to changes in electrical flame-off (EFO) (FAB diameter relative standard deviation: 0.94; ball-to-wire offset: 0.53 μm) [57]. Comparisons of bare Cu and PdCu wire have shown that at a higher EFO current, an FAB with bare Cu wire has higher hardness caused by having smaller grains. Varying the EFO current in PdCu wire causes the hardness of the wire to vary due to the different distributions of the PdCu alloy in the FAB [58].

Although Pd coating prevents the oxidation of Cu, it introduces new challenges for wire bonding. It is 2.5 times more expensive than bare Cu [59] and has a higher melting point than Cu [59]. The industry is thus looking to optimize Pd thickness to reduce costs, decreasing the Pd thickness from 0.2 to 0.1 μm [54]. PdCu is harder than pure Cu and, hence, increases the risk of pad cracking and damage to the circuitry under pad (CUP). The Pd distribution can also affect the reliability of Cu wire-bonded devices, but as of 2013 there was no method to control Pd distribution.

2.2 Oxidation Prevention Technology

FAB formation requires the generation of high voltage across the EFO gap, causing a high current spark to discharge and melt the tail of the Cu wire to form a spherical ball. Oxidation must be avoided in order to obtain a symmetrical FAB without deviation in size [60]. Cu oxidation during ball formation inhibits the formation of a spherical ball, which in turn affects the reliability of the first bond. Under high-temperature and high-humidity environments, copper oxidation at the interface of the Cu–Al bonding region causes cracks and weakens the Cu–Al bonding. Copper oxidation typically starts at the wire region and then spreads to the upper bonded area and then to the bonding interface with time. Cu oxidation also causes corrosion cracks.

Since Cu oxidizes quickly, Cu FABs need to be formed in an inert gas environment. Oxidation can also occur if the cover (inert) gas flow rate is not sufficiently high to provide an inert atmosphere for the FAB formation [61]. It has been reported that the use of single-crystal Cu wires eliminates the need for cover gas during bonding [62]. Requiring inert gas, such as forming gas, to address the oxidation problem adds complications to the bonding process and results in a narrow process window.

The oxidation of Cu is prevented in two ways: use of an inert gas (nitrogen or forming gas) during bonding, and use of oxidation prevention coating on the Cu wire [42, 63, 64]. The use of N_2 as the cover/shielding gas has resulted in defective FABs. Since forming gas contains 5 % H_2 (95 % N_2, 5 % H_2), it has better anti-oxidation properties than N_2 and is the cover gas for Cu wire bonding. The main purpose of injecting forming gas (FG) is to form an inert gas shroud around the copper tail and the FAB to prevent oxidation prior to bonding. The use of H_2 has the twofold purpose of helping to melt the Cu, as well as acting as a reducing agent to reduce the copper oxide back to Cu [60].

2.3 Free Air Ball Formation

FAB formation starts with the Cu wire being heated and subsequently melted by the low-energy plasma discharged. The molten wire turns into a spherical ball under the effect of surface tension. At the end of discharge, the molten spherical ball starts cooling and then solidifies to form a FAB [65]. Qin et al. [66] compared Au and Cu balls on Al pads and found that non-optimized bonding conditions resulted in over-bonded balls for Au wire and under-bonded balls for Cu wire. Although Cu wire bonds showed higher pull strength than Au wire bonds, Cu wire bonds had a larger standard deviation, which indicates that more process development is required to optimize the process conditions for Cu wire bonding. Figure 2.2(a, b) shows the FAB micrographs for Au and Cu wires. Even though the ball diameter of Au wire (39 μm) was higher than that of Cu wire (37 μm), the volume of the bonded ball was found to be lower in the case of Au. One possible reason is the softness of Au, which makes Au able to be more easily squeezed into a capillary during the plastic

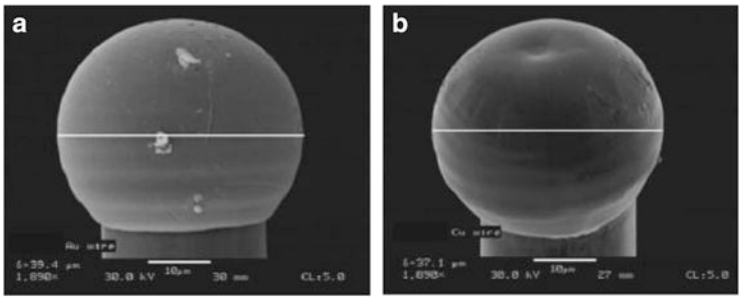

Fig. 2.2 Free air ball (FAB) diameter comparison (**a**) Au wire: 39 µm, and (**b**) Cu wire: 37 µm [66]

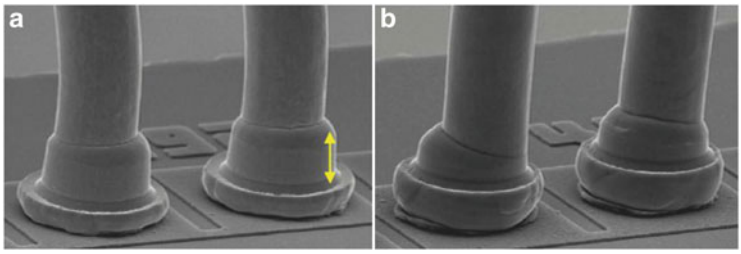

Fig. 2.3 (**a**) Bonded balls with Au wire, showing a higher height than Cu wire due to a lower bonded ball volume/FAB volume ratio (33 %); (**b**) bonded balls with Cu wire, showing a lower height compared to Au due to a higher bonded ball volume/FAB volume ratio (64 %) [66]

deformation process compared to the harder Cu. The ratio of bonded ball volume to FAB volume was found to be 33 % for Au and 64 % for Cu. This difference is significant, indicating that most of the FAB was captured inside the capillary for Au wire, whereas for Cu wire, most of the FAB was outside the capillary as a bonded ball. A lower ratio of bonded ball volume to FAB volume results in a taller ball bond for Au wire compared to Cu. The Cu FAB should be made smaller than Au FABs.

Another damage mechanism related to the bonding process is known as Al splash, which is defined as the amount of material displacement outside the bonded ball contact perimeter. Al splash should be minimized, as it can result in shorts with the neighboring terminals. In the case of bonding with Cu or Au wire, the FAB hardness of Cu is 80 HV and for Au it is 60 HV. The bonded ball hardness for Cu is 100–128 HV, whereas for Au it is 70–80 HV. The bond hardness of Cu is higher than the bond hardness of gold due to the strain hardening effect. The hardness of Al is 70–80 HV, which is similar to Au and much lower than Cu, explaining why more splashes were observed while bonding with Cu wire (Fig. 2.3a, b) [66].

The outside edge of the FAB has been found to be harder than the inside of the FAB, since it experiences higher stress and strain during the bonding process [66]. Solutions to minimize the stress on the pad include decreasing the normal force, decreasing the sliding distance, and increasing the hardness of the pad. One way to

increase the hardness of the pad is to use alternative pad metallurgies, including NiPdAu or NiAu. Qin et al. [66] showed the excellent robustness and reliability performance of the Al pad surface in bonding with Cu wire and eliminating Al splash.

2.4 First (Ball) and Second (Wedge) Bond

The formation of a first bond requires deformation of the FAB on the heated substrate by the application of ultrasonic energy and bonding force. The bonding force leads to work hardening, while the ultrasonic energy softens the wire. On the other hand, the second bond is formed by deformation of the wire by the application of bonding force and ultrasonic energy, where the initial microstructural state of the wire governs the wire deformation during bonding. The formation of second bonds has been a challenge with Cu due to its high stiffness and tendency to work harden. The problem is exacerbated by the presence of an oxidation layer on the bare Cu surface, which reduces the wire bondability. Atomic emission spectroscopy conducted on Cu wires in the initial state prior to bonding has showed the presence of copper oxide (Cu_2O) [50]. The formation of copper oxide must be limited by the use of organic coatings on the wire. Additionally, plasma cleaning, typically argon plasma cleaning, must be performed on all substrates within 8 h of wire bonding [54].

The parameters generally optimized for second bonds are ultrasonic bond power (P), bond force (F), and bond time (T). Fujimoto et al. [67] reported the optimization of bonding force and ultrasonic energy for second bond formation. They controlled the wire deformation by varying the bonding force during the initial touchdown phase (initial deformation), as well as during the ultrasonic deformation. They reported that for a 30 μm, 5 N Cu wire, the optimal force during the initial deformation period was 1.4 N, and during the ultrasonic application was 0.4 N.

Cu wire bonding has low units per hour (UPH) because of the longer bonding time for the formation of first and second bonds, compared to Au wire bonding. Mechanical limitations such as heat profile delays, mechanical motion delays, and bonding delays introduce additional delays in the bonding time. Process and bonding time optimization need to be carried out to improve the UPH. A low mean time between assist (MTBA) is mainly caused by non-sticking and short tail. Appelt et al. [68, 69] reported successful implementation of fine-pitch Cu wire bonding in high-volume manufacturing (HVM), where the quality and yield were equal to those of Au wire bonding. Those Cu wire-bonded parts exceeded the standard JEDEC reliability testing specifications by twice the recommended amount. Also, as discussed in section "Bond Wire," palladium-coated Cu wires are being adopted to address the problem of second bond formation with Cu wire due to the reduced oxide formation at the wire surface.

The formation of stitch bonds on quad-flat packages (QFPs) is a challenge for Cu wire bonding. Ultrasonic energy cannot be used for the stitch processes on QFP packages due to the resonant condition of the lead beams that causes wire fatigue and breakage. A thermocompression scrub is used instead, with a combination of force and low-frequency X–Y table scrubbing [54]. For Cu wire bonding on

pre-plated lead frames, the low strength of second bonds, which is related to the cold forming (high-speed forging process) of Cu wire, is a challenge. Bing et al. [70] conducted vacuum heat treatment of samples at 200 °C for 10 min, followed by wire pull tests and microstructure observations. Deformed grains in the second bonds went through a recovery process, resulting in the bonding strength of the second bonds exceeding the Cu wire strength.

2.5 Wire Bond Process Parameters

The bonding parameters that affect the quality of the formed FAB and the first and second bonds are discussed in this section.

2.5.1 Ultrasonic Energy

Ultrasonic energy is one of the wire bonding processing parameters that determines the bond strength and reliability [27, 55, 71–74]. During the bonding process, the application of bonding force work hardens the bonding wire. Additionally, the high hardness of Cu introduces the risk of underpad damage due to the requirement of higher bonding force. The use of ultrasonic energy lowers the bonding force in bonding by softening the FAB. The ultrasonic energy increases the dislocation density, lowering the flow stress and increasing the wire softness. Thus, the application of ultrasonic energy lowers the wire deformation required for bonding.

Ultrasonic power is directly proportional to bonding wire softening, which in turn determines the bond quality and appearance. Figure 2.4 shows the different failure modes and their occurrence with increasing ultrasonic power for a constant bonding time and force (30 ms/0.392 N). At a lower ultrasonic power, the failure mode is a break at the bond–pad interface. The failure mode shifts to neck break and bond break as the ultrasonic power increases [75].

The optimum ultrasonic power should be determined to achieve good bond quality [71, 76]. Insufficient power has been shown to cause under-formed bonds and tail lifts; however, excessive power can cause a squashed appearance, cracks, and/or cratering damage to the underlying structure on the semiconductor die, resulting in damaged joints [16]. The bondability of copper wire can be determined by the slip area at the bonding interface. The transfer from the slip area to the entire slip can be controlled by the levels of the ultrasonic power and bonding force used. The initial temperature of the preheated chip can also improve the bonding strength [77]. Huang et al. [71] investigated the effect of ultrasonic energy on FAB deformation. He reported that the required ball height can be obtained by lowering the bonding force and increasing the ultrasonic power. This in turn can reduce the stresses on the underpad structure and reduce the possible pad damage. Huang et al. [71] reported that for a ball height of 45 μm (for 50 μm wire), the bonding force decreases linearly as the ultrasonic power increases.

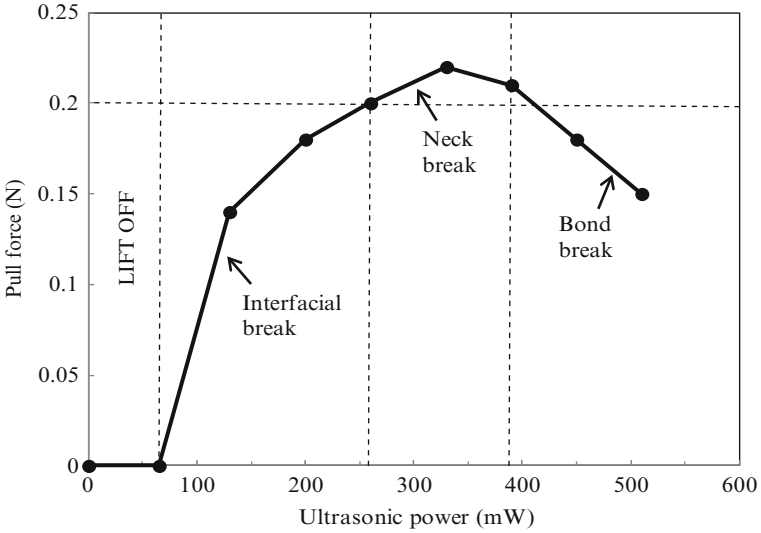

Fig. 2.4 Shift in failure modes as a function of increasing pull force and ultrasonic power (mW) [75]

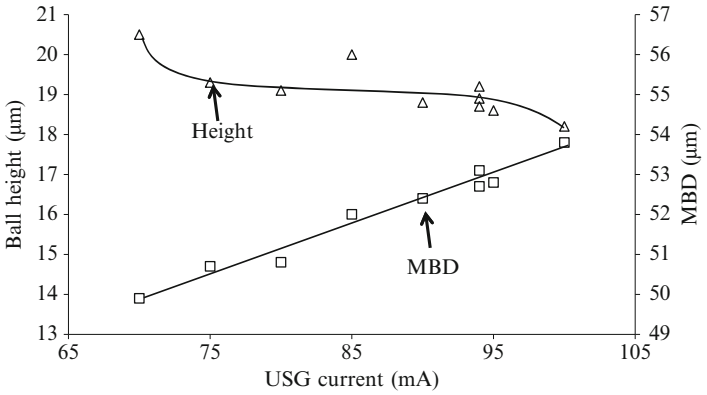

Fig. 2.5 Effects of ultrasonic generator (USG) current on ball geometry [55]

Also, the degree of ultrasonic softening at an ultrasonic power was directly proportional to the ultrasonic amplitude.

The USG current settings must be optimized to achieve good ball bonds. Hong et al. [76] carried out optimization of the bonding ultrasonic power for Cu–Al bonding of Cu wire of 23 μm bonded onto 3 μm thick aluminum–1 % silicon metallization, and reported the optimized ultrasonic energy to be 100 mA. Optimization requires measuring the deformed ball diameter. Zhong et al. [55] reported that, out of all the bond processing parameters, USG current had the most significant impact on ball deformation (mashed ball diameter (MBD)) and reduction in ball height (Fig. 2.5).

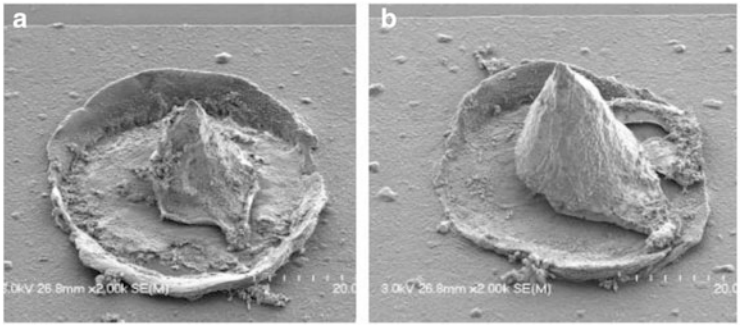

Fig. 2.6 SEM micrographs of Al pads after etching away of the bonded Cu balls: (**a**) 0 % pre-bleed: more pad splash and pad damage at the edge; (**b**) 100 % pre-bleed: less pad splash and pad damage [66]

It has been reported that USG current increases bonded ball diameter, ball shear force, and shear force per unit area, and decreases ball height [45, 55]. The shear force per unit area represents how well the micro-weld has been formed between the copper ball and its Al bond pad on an IC chip. When the USG current increases, the shear force per unit area initially increases, saturates over a range, and then increases again. This result suggests that there is an optimum USG current setting in the saturation region of the shear force per unit area. A higher shear force per unit area can be achieved by increasing the USG current (65–105 mA), but this can also cause cratering on the Al bond pad of the IC chip. The optimum USG current should be determined to achieve good copper ball bonds. Clauberg et al. [78] reported the optimization of ultrasonic energy for Cu wire bonding to Al pads based on the Al splash diameter since the Al splash diameter was 4 μm greater than the ball diameter. Additionally, for NiPdAu surface metallization, higher ultrasonic energies could be used at a pitch of 50 μm and upper limit of 40 μm for the ball diameter. Also, ultrasonic energy of up to 115 mA could be used without damaging the underpad structure. In comparison, for bare Al pads, the maximum ultrasonic energy that could be used was 85 mA for 50 μm pitch and 40 μm ball diameter. Ultrasonic energy has been optimized to reduce the underpad stress by reducing the Al splash [27, 71, 73, 74].

Pre-bleed ultrasonic energy is the energy before the impact and is activated when the bonding tool (capillary) achieves the required height. It is applied from the start of contact to the end of impact. If the ultrasonic energy is applied in conjunction with the bonding force during the initial formation and deformation of the FAB, the Cu becomes softer and the ball height becomes less than it would be in the absence of ultrasonic power. Researchers have investigated the use of pre-bleed energy to reduce the underpad stress [71, 74]. Designs of experiment (DOEs) conducted to analyze the effects of pre-bleed have indicated that high pre-bleed settings (>100 mA) decrease Al splash at the edge of the ball [66]. Pre-bleed helps to maintain a flat ball and pad interface, eliminating the concave shape that occurs when pre-bleed is not used (Fig. 2.6). A concave shape is undesirable, since it indicates pad wear near the edge of the bond and poor bonding at the center of the ball. Pre-bleed USG propagates

ultrasonic scrubbing from the ball center to the edge. Other advantages of pre-bleed include elimination of the thinning ring of the Al pad and enabled use of low ultrasonic energy (<90 mA).

2.5.2 Electric Flame-Off Current and Firing Time

EFO current is supplied to form an FAB [79] during the first step in the wire bonding cycle. The heat-affected zone (HAZ) is the wire portion near the ball that undergoes annealing during the firing process. The length of the HAZ depends on the magnitude of the heat-flux during the firing process. Under heat, the grains in the HAZ grow, and as a result, they have different mechanical properties than the rest of the wire. The HAZ affects the wire loop height, wherein a lower HAZ is required to attain a lower loop height. The EFO current and firing time must also be optimized to minimize the HAZ. As the EFO current and firing time decrease, the HAZ length decreases. With the increase in current, the arc duration required to form the FAB decreases. The decrease in arc duration, in turn, results in less available time for the effect of heat to penetrate axially along the wire away from the ball. Since the metal has a finite diffusivity, the length of penetration of the heat effects decreases with higher currents [80]. It has been reported that an increase in the EFO current reduces the HAZ length and increases the deformability of the ball [65, 81, 82]. Zhong et al. [55] reported that a FAB with a higher EFO had a Vickers hardness (HV) that was 9.28 lower than that with a lower EFO (120.82 HV vs. 114.26 HV). Hang et al. [65] reported that up to an 8 % reduction in the underpad stress can be obtained by using high EFO current combined with short firing time. The EFO current combined with superimposed ultrasonics affects the deformation of PdCu wires [83], where higher current leads to more deformable balls and increases the variation in FAB size and shape, and lower EFO current leads to less variation but higher FAB hardness. The use of ultrasonic energy along with the bond force results in a reduction in the force required for FAB deformation.

The micro-hardness of bonded Cu balls is related to the EFO parameters with softer FABs obtained by higher EFO current. This lower hardness is attributed to the higher maximum temperature during FAB melting due to the high EFO current. Because EFO current and EFO firing time are closely related, it is more appropriate to use firing time as a hardness index for FABs. This would make it less dependent on the diameter of the Cu wire. Therefore, for Cu wire bonding, to achieve a soft FAB and minimize the stress induced during ball bond impact, it is recommended to have a shorter firing time during FAB formation, use a lower contact velocity to minimize the impact stress, and use a higher gas flow rate to provide sufficient inert gas coverage to avoid pointed FABs [55].

The EFO parameters, such as EFO current, FAB diameter, EFO gap length, and cover gas flow rate, have to be optimized for Cu wire bonding [20, 55, 61, 84].

FAB requirements include ball size repeatability (the relative standard deviation (standard deviation/average diameter) < 1–1.5 %), ball-to-wire offset for bonded ball concentricity, and no malformed balls (e.g., pointed or oxidized) [54].

The FAB hardness affects the bondability of the FAB: the harder the FAB is, the more difficult it is to form the ball bond. The FAB hardness, in turn, is determined by the cooling rate during solidification of the FAB. During the solidification and cooling of FABs, a large amount of heat is lost by conduction up the wire, and the heat loss is proportional to the cross-sectional area of the wire. An increase in the EFO current coupled with a decrease in EFO time results in a high FAB temperature and thermal gradient across the FAB and unmelted wire. The resulting FAB has a higher residual stress, dislocation density, and, therefore, hardness [85].

The wire diameter variation affects the ball diameter, but it is not controlled in Cu wire bonding. In general, the ratio of FAB diameter to wire diameter should be between 1.6 and 3, depending on the wire diameter, EFO current, and firing time [54]. A higher EFO current leads to better ball size repeatability but a lower number of concentric balls. The optimal settings for the EFO gap depend on the flow head design. A higher gap provides better ball concentricity. The cover gas flow rate also affects the formed ball [61, 86], in that a low rate results in oxidized balls, whereas a high rate results in pointed balls. Based on the wire diameter and type of EFO current, the gas flow rate should be optimized.

For PdCu wires, a larger diameter wire typically has a thicker Pd layer compared to wires with smaller diameters. As the wire diameter gets smaller, the PdCu solid-solution protective layer on the bonded ball becomes thinner. Therefore, there is a higher tendency for smaller wires to have more exposed Cu regions on the bonded balls than larger wires [87]. To ensure protection of first bonds against HAST and PCT, the Pd in PdCu wire has to be distributed over the entire surface of the FABs, forming a protective shield against corrosion attack by halogen ions in molding compounds. Various PdCu wires may have different Pd layer thicknesses over the Cu cores. FABs of different PdCu wires behave differently under the same EFO conditions. Unlike bare Au and bare Cu wires, the FAB formation in PdCu wire has to be optimized individually and is not interchangeable among different PdCu wires. If the EFO parameters are not optimized, dimple FABs and/or inconsistent FABs will be formed [88]. The nonuniform distribution of Pd in the first bonds and the voids associated with Pd-rich phases may contribute to the increase of resistivity and temperature, influencing the formation of intermetallic compounds. Also, the copper ball bond is harder in Pd-rich regions [89].

In Cu wire bonding, the standard FAB diameter is typically 2–2.5 times greater than the wire diameter. More energy is needed to melt the copper tail to form a standard FAB ball, as compared to Au wire bonding. Hang et al. [90] investigated the FABs formed under different EFO conditions (Fig. 2.7). They reported that the FAB formed by Cu wire of 50 μm diameter with an EFO current below 120 mA did not meet the FAB requirement of symmetrical shape and surface. The symmetricity of the FABs was defined as the ratio of D_A and D_B as shown in Fig. 2.7.

One of the causes of FAB defects is nonhomogeneous cooling or oxidation. Cu wire requires higher EFO current than Au wire. The resulting higher temperature could cause a sudden expansion of the forming gas around the FAB. During the wire bond cycle, if the forming gas supply is insufficient, the oxygen surges into the glass tube through the hole where the capillary passes, resulting in oxidation of the FAB [91].

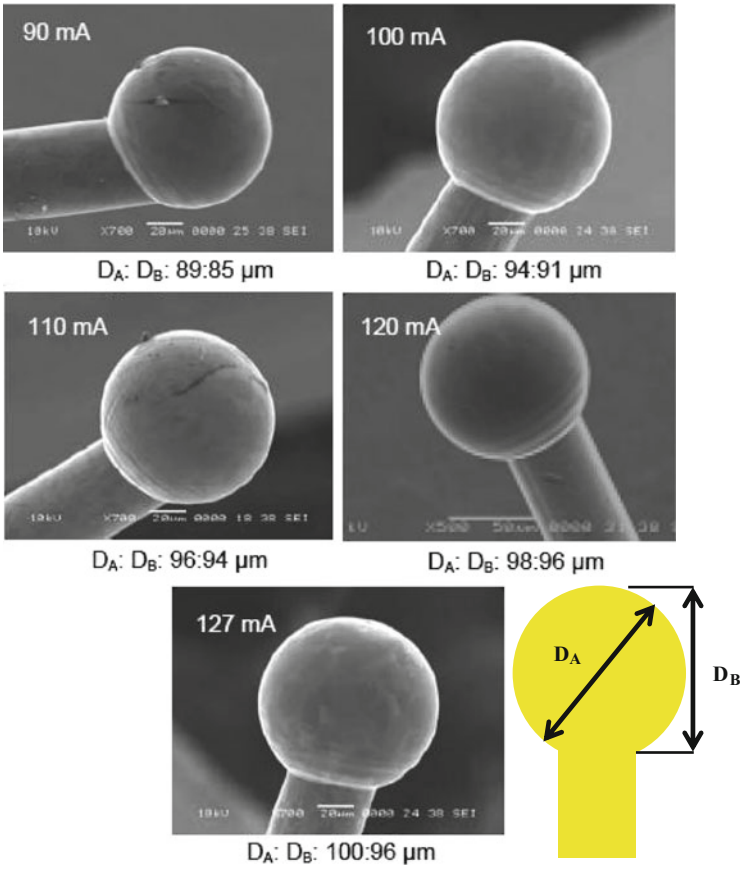

Fig. 2.7 SEM images of Cu FABs formed with different EFO current settings (90–127 mA) [90]

A slow flow rate causes an asymmetric shape of the FAB [85] and thus is unacceptable from a reliability standpoint [90], as shown in Fig. 2.8.

Pequegnat et al. [85] investigated the effect of gas flow rates and reported that the convective cooling effect of the cover gas increased with a flow rate up to 0.65 l/min, and the EFO site showed a 19 °C decrease in temperature. Flow rates higher than 0.71 l/min result in FAB oxidation due to the change in flow from laminar to turbulent. The addition of hydrogen to the cover gas reduces the oxidation of the FAB and provides additional thermal energy during EFO. Jiang et al. [91] carried out an experiment to optimize the forming gas flow rate and EFO settings to target Cu FABs that were 45 µm in diameter. They reported the optimum gas flow rate to be 0.5 l/min. A flow rate lower than the optimum level leads to partially oxidized and distorted FABs. A flow rate higher than the optimum level (0.5 l/min) leads to a strong convection effect, leading to pointed balls. Based on the wire diameter and type, the EFO current and gas flow rate should be optimized.

In a study by Stephan et al. [58], the comparison of bare Cu and PdCu wires showed that at a high EFO current setting (60 mA for FAB diameter of 40 µm and

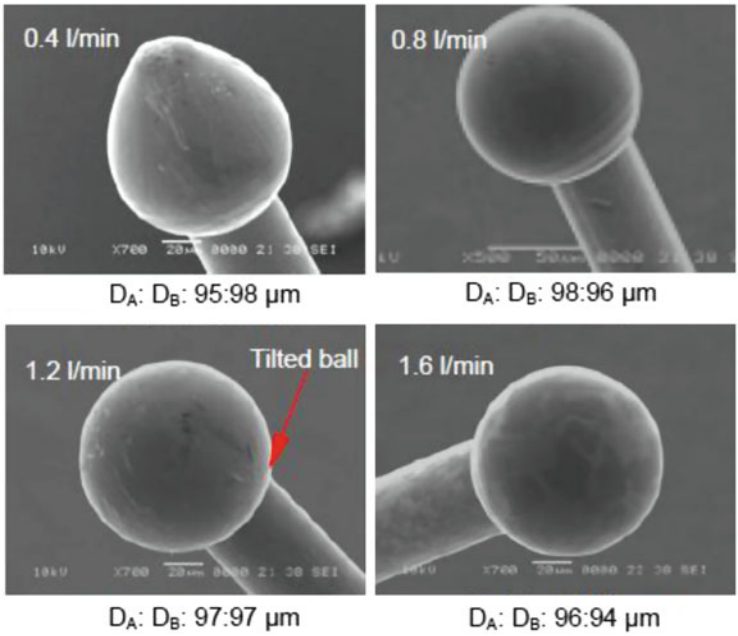

Fig. 2.8 Cu FABs formed at different inert gas flow rates [90]

wire diameter of 20 µm), FABs with bare Cu wire have higher hardness than PdCu wire caused by having smaller grains. For PdCu wire, varying the EFO current (30, 60, and 120 mA) varies the hardness because of the different distributions of the PdCu alloy in the FAB [58]. The dependence of the Pd-distribution on the EFO current suggests that the temperature rise during the EFO current firing is high enough to soften the Pd and cause it to distribute around the FAB, but the temperature is lower than the melting point of Pd (1,554.9 °C). To investigate the presence of Pd, analytical methods, such as energy-dispersive X-ray spectroscopy (EDS), can be used. Another way to investigate the presence of Pd is to use a chemical etching solution such as ferric chloride ($FeCl_3$) to etch away the Cu and leave the Pd. Several reports have been published to investigate the presence of Pd in the FAB and at the bond–pad interface [58, 92], but limited studies have been conducted to investigate the effect of Pd concentration mapping on bonding strength or the effect of EFO on bonding strength.

A comparison of N_2 and forming gas for PdCu wire (15 µm) showed that forming gas is superior to N_2, since it is not sensitive to changes in EFO (FAB diameter relative standard deviation = 0.94; ball-to-wire offset = 0.53 µm) [54]. When comparing the FAB strength for Cu and PdCu wires bonded in nitrogen or inert gas (forming gas), no significant difference was observed between the two gases for similar EFO currents and energies [93], as shown in Fig. 2.9. It was reported that nitrogen requires 5 % longer than inert gas to achieve the same FAB size. Comparing ball lift, only a minor difference was observed when bonding Cu and PdCu wires in nitrogen or inert gas (Fig. 2.10).

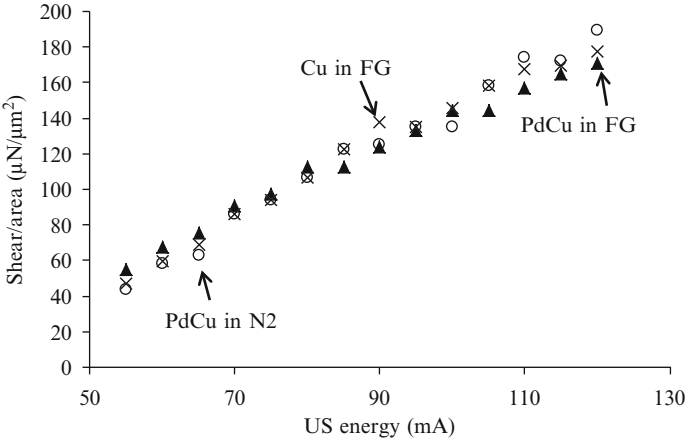

Fig. 2.9 Shear strength for PdCu wire bonded in nitrogen or forming gas [93]

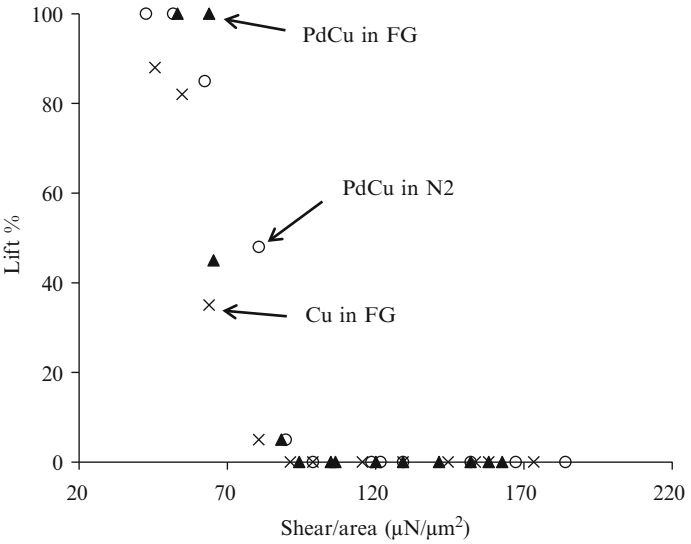

Fig. 2.10 Ball lifts for Cu and PdCu wires bonded in nitrogen or forming gas [93]

2.5.3 Bond Force

The bond force is the downward force exerted by the bonding head during bonding. The bond power is optimized along with the bond force. An increase in bond force and power allows for proper coupling of ultrasonic energy between the bond wire and pad metallization. As mentioned earlier, Cu wire is stiffer than Au wire, which results in higher bonding force requirements compared to Au wire [94, 95].

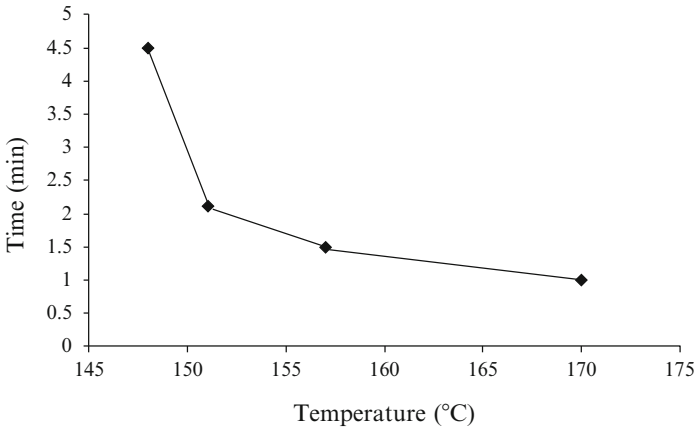

Fig. 2.11 Bonding temperature vs. Cu pad exposure duration [98]

A high bonding force transmits high force onto the bond pads, which is not desirable, since it can damage the pad or cause pad cratering [16]. On the other hand, a low bonding force leads to the nonstick-on-pad (NSOP) condition [96]. Hence, optimization of bonding force needs to be carried out. Hong et al. [76] reported the optimized bond force for shear strength to be 0.589 N for a 23 μm Cu wire with an elongation range of 8–16 % and a break load range of 0.059–0.118 N on a silicon chip $1.06 \times 1.26\,mm^2$ in size, sputtered with 3 μm thick aluminum containing 1 % silicon.

2.5.4 Bonding Temperature and Time

Bonding temperature contributes to the reliability of the resulting bond. It softens the wire and thus improves the deformability of the wire for bonding. Temperature also affects the deformability of the FAB, which solidifies over a heated substrate. It increases the diffusion at the FAB–bond pad interface. However, high temperatures can result in rigidity loss for board materials, causing bonds to lift due to "ultrasonic cupping." Ultrasonic cupping occurs when the bonding wire slips out from the contact area between the board plating and the bonding wire during wire bonding. Lee et al. [97] reported a substantial increase in tail bond force and pull force for Cu wire on silver metallization due to a bonding temperature increase from 120 to 240 °C. In another study Hong et al. [76] reported the optimized bonding temperature (for shear strength) to be 220 °C for 23 μm Cu wire with an elongation range of 8–16 % and a break load range of 0.059–0.118 N on a silicon chip with 3 μm thick Al–1 % silicon. The bonding temperature is also known to affect the bondability of the Cu wire [98]. A ball bond was formed on a Cu pad at an interval of 15 s, and the bonding was continued until a no-stick occurred due to the oxidation of Cu pad. At the same time, the bonding stage temperature was varied from 145 to 170 °C (Fig. 2.11). The pad exposure time was an indicator of oxidation time. As seen in

Fig. 2.11, at a bonding temperature of 145 °C, no nonstick was observed even after a pad exposure of 6 min.

Many times, the bond pad temperature is not provided in the literature and the substrate stage or heater plate temperature is specified instead, which is higher than the actual bond pad temperature. For example, Shah et al. [98] measured a bond pad temperature of only 138 °C at a table temperature of 150 °C. As reported by Ramelow [45], comparing bonding temperatures across the literature is difficult because of the difference in the package geometries and thermal conductivities.

Bond time is the duration of the applied ultrasonic energy and bond force. Time has the widest process window; however, excessive bond time can result in slow throughput in manufacturing lines, increased tool maintenance due to contamination buildup and wear, and damaged or burnt appearing wire bonds in areas where the tool contacts the bond.

The optimized parameter values are dependent on various factors, including the wire diameter, pad material, and pad surface cleaning. For a 25 μm Cu wire on Al metallization, the optimized parameters are a bonding force of 0.157 N, a USG current of 90 mA, and a bonding time of 15 ms [22]. Whereas for 23–25 μm Cu wire on an Al pad, the optimized parameters were a bonding force of 0.245–0.451 N, US power of 110–130 mW, and bonding time of 9–10 ms. England et al. [28] reported the bonding parameter-optimized values for a 25 μm Cu wire bonded to Al–0.5 % Cu. The optimized values were a bond force of 0.167–0.334 N, USG power of 90–120 mW, and bonding temperature of 150–175 °C.

2.6 Bonding Process Optimization

The process window for Cu wire bonding is narrower than for Au wire bonding [29]. A good process window for Cu wire bonding can be achieved by designing an experiment that is tailored to the Cu wire bonding process. Bond parameter optimization is aimed at carrying out bonding with no pad cratering or cracking, and 100 % ball bond containment within the pad that is lower than the surrounding metal. Tight capillary control is required to reduce the variation in ball size and facilitate HVM. Another part of process optimization is to obtain adequate IMC coverage [99, 100]. In order to maintain yield, the pad metallization should be cleaned using plasma cleaning to prevent the ingression of foreign particles on the die and substrate prior to bonding.

Process optimization ensures bonding process stability and defines a process parameter window for first and second bond quality [101]. Researchers have adopted several methods for process optimization of Cu wire bonding such as Taguchi methods [102], Six Sigma “define–measure–analyze–improve–control” (DMAIC) methodology [103], orthogonal response surface methodology (RSM) [91, 104, 105], and statistical DOE [105].

Cu wire bond process optimization is essential for bond process stability and the portability of machines and materials. Optimization experiments are conducted to determine the mathematical relationship between the variables and to center the process.

Process centering is also known as finding the process window. The effects of normal process drift can be minimized by centering the process within an acceptable window [106]. Process optimization defines a process parameter window for first and second bond quality.

The common statistical techniques for optimization of the bonding process are DOE, RSM, and contour plots. Wong et al. [105] defined statistical DOE as a way to "encompass methods for the planning, design, data collection, analysis and interpretation of experiments that enables one to effectively and efficiently build the bonding process and use a statistical model between experimental responses and controllable factor inputs." A DOE helps to determine the most important variable(s) for a process. The center point is a statistical method to determine any possible process drift or instability by providing an estimate of the experimental error. RSM is another technique that is used to determine the optimum empirical relationship between a set of input variables and responses. A combination of DOE and RSM methodologies can optimize the bonding parameters. Contour plots can be used to observe the relation between two input factors and the responses [105].

Researchers have conducted statistical DOE and RSM on common bonding process parameters, such as contact velocity (C/V), bond power, bond force, USG current, and bonding time, to determine the factors affecting the process [91, 105]. Jiang et al. [91] investigated the process window development for Cu wire bonding based on contact velocity, initial force, bond force, USG current, and bonding time. The DOE was carried out based on those input factors, and the response factors were wire pull strength, ball shear strength, and cratering performance on bond pads. The DOE study adopted a half fractional DOE with five input factors to look for factors affecting the model. Based on the results, three factors were chosen for advanced DOE with RSM to obtain the final optimum parameter range.

Wong et al. [105] conducted a DOE to optimize the process parameter window to achieve a ball bond with targeted bonded ball diameter (BBD), bonded ball height (BBH), wire pull, and ball shear strength. The DOE was conducted on bond power, bond force, and bond time to determine the "significant parameters" affecting the process parameter window. The response surface comprised BBD, BBH, wire pull, and ball shear strengths. After the initial screening, full factorial design to determine the interactions between the two significant parameters, bond power and bond force, was conducted. The RSM matrix was used to determine and model the optimum region. Based on the study, bond power was found to be the critical factor in reducing bonded ball diameter.

As an example of bond process optimization (Fig. 2.12), the process window at K&S is determined by the acceptable IMC coverage (generally 80 % or more), Al splash (should not reach the passivation layer), pad crack, and failure site under the pull test (no ball lift or pad peel). It can be seen that Cu wire bonding has a narrow process window due to those considerations.

Su et al. [102] demonstrated the application of Taguchi methods for process optimization and increased the yield from 98.5 to 99.3 %, saving USD $700,000. Lin et al. [103] used the Six Sigma DMAIC methodology to optimize the material, machine, and bonding parameters, developing a new bonding method of flattening

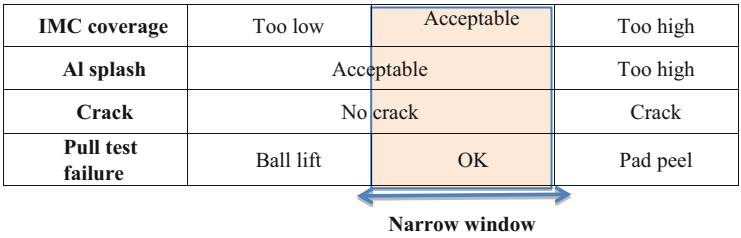

Fig. 2.12 Process window for Cu wire bonding [54]

the bonded ball and applying gentle ultrasonic operation. They also reported that the capillary design and surface roughness improved the wire bond response. Wire coupling with optimum electrical firing parameters and air cushioning can help to achieve robust and oxidation-free FABs.

In addition to bonding parameter optimization, process control for Cu wire bonding manufacturing conditions has to be conducted. Teck et al. [107] conducted a wire floor life control study to determine the usable life of Cu wire after unpacking it from a wire supplier's seal with inert gas. The capillary touchdown limit for a 47 μm bond pad pitch with a wire size of 20 μm was determined. Capillary degradation started at 200k touchdown, and buildup at the capillary sidewall started at 300k touchdown, causing tail short conditions. Staging on a heater block was also studied to determine the reliability and manufacturability due to substrate outgassing during wire bond heating. The die bonded unit was staged on top of the wire bonder heater block for 0, 15, and 30 min to simulate a scenario where a unit was left on a wire bonder heater until the machine stopped. It was found that substrate outgassing did not affect the manufacturability. The wire pull and ball shear strength showed a reduction after 15 min of staging, but an improvement after 30 min of staging. The improvement was attributed to the interfacial IMC growth due to 30 min of heating at 170 °C. Another way to improve the adhesion of Cu–Al after bonding is to enhance intermetallic growth by heat treatment [108].

Process optimization can improve the bond reliability of specialized die structures such as overhang dies [109, 110]. Kumar et al. [109] demonstrated the process characterizations of different overhang die configurations, where a process was developed for consistent ball shape, remnant Al underneath the bonded ball, and looping across the overhang area. Li et al. [111] developed an approach to reduce the bonding impact on the die by increasing the thickness of the Al pad from 1 to 2.8 μm. The micro-hardness of the bond pad structure decreased by three times, leading to a reduction in the impact and rebound force. The shear strength of Cu wire overhang showed an improvement in the shear strength.

In the process optimization approach followed by K&S, a model-based response-driven approach is adopted, wherein a numerical model is derived from extensive process testing, and bonding parameters are scaled for ball diameter. In order to develop the pitch model for Cu wire bonding, the target ball diameter is set and the bonding accuracy and Al splash are taken into account. After this, the wire

Table 2.3 Optimized capillary, wire and bond dimensions (μm) [54]

Wire Dia	Cap Hole	Cap Chamfer Dia (CD)	Min. Bonded Ball Dia
15	19–20	23–25	27
*20	*24–28	*28–35.5	*36

*most common

size is chosen. Cu is 2.54 μm thinner than Au for the same pitch because of Al splash. Table 2.3 shows an example of the optimized dimensions of a capillary, wire, and bond, as chosen by K&S for Cu wire bonding.

The requirements to achieve quality first and second joints are optimized process parameters, an optimal bonding environment, a contamination-free surface, and proper maintenance of the tool MTBA. The bond pads on an active circuit or a CUP can be damaged if the bonding parameters are not optimized. The main challenges, as mentioned in Chap. 8, are hardness and oxidation. The bonding process needs to be optimized, and parameter adjustments must be made for power, pre-bleed energy, USG current, EFO current, force, and temperature for the Cu wire bonding process. The optimum power should be determined to achieve good bond quality. With increasing ultrasonic power, shear, but not diameter, should increase. The optimum USG current should be established to achieve a uniform ball bond, as the ball deformation and ball shear force increase with an increase in USG current.

2.7 Bonding Equipment

Cu wire bonders require enhanced capability for bonding force and cover gas consumption control. Ramelow et al. [45] reported that bonding companies have developed in-house bonders tailored for Cu wire bonding. For example, ESEC's range of bonders includes the 3100 optima Cu. Similarly, K&S built the Cu wire bonder IConnPSProCu, which contains new, customized hardware with an optimized gas feeding system and high-performance process control. The cover gas feeding system enhances the process window while at the same time reducing the cover gas consumption. Similarly, ASM also provides an automatic wire bonder for Cu wire bonding, Eagle 339Cu, which can bond both fine-pitch and thick wires. The bonder has a special kit to prevent oxidation and has been optimized to minimize the need for forming gas. Cu wire bonding is carried out either with the ball bonder retrofitted with a Cu kit, such as in ESEC (COWI-2), which can perform both Au and Cu wire bonding. The Cu kits contain the system for spooling the wire spools in pure nitrogen and equipment to provide efficient overpressure atmosphere of the forming gas. For example, the ESEC COWI-2 kit is equipped with forming gas flow controls and pressure sensors to keep a check on the gas pressure and flow. Recently, the wire bonder kits include Cu kits such as iConn, the Maxum Ultra, the MaxumPlus, and the 9028 PPS. Other bonders being used are the automatic bonder Eagle 60AP with 138 kHz and the K&S Nu-Tek bonder.

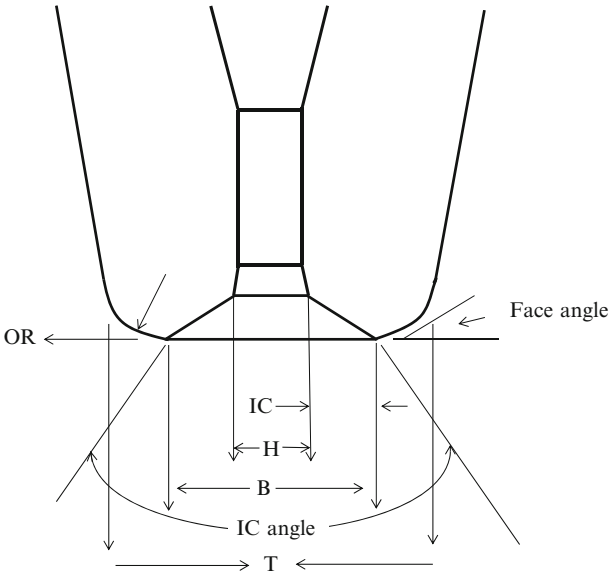

Fig. 2.13 Capillary tip geometry dimensions (tip diameter (*T*), hole diameter (*H*), chamfer diameter (*B*), inside chamfer (IC), inside chamfer angle (IC angle), and outside radius (OR) [112]

In wire bonding, the necessary bonding force and ultrasonic energy are transferred to the wire and the bonding pad/substrate by the capillary to form the bonds. Figure 2.13 shows a schematic of a capillary used in wire bonding. The capillary tip geometry dimensions, including tip diameter, hole diameter, chamfer diameter, inside chamfer, inside chamfer angle, and outside radius, are shown.

The hardness of copper wire is approximately 25 % higher than gold wire, and thus, it is more difficult to bond, especially for lead frame devices. To improve the stitch bondability, higher parameter settings are used for Cu wire than for Au wire, causing heavy cap marks and potential short tails or wire opens. Due to the requirement of higher bonding parameters in Cu wire bonding, the capillaries in Cu wire bonding have short lifetimes: 1000k touchdowns for Au bonding vs. 400k touchdowns for Cu [45]. In addition, Cu–Au stitch bonds are weak. Therefore, copper wire bonding has wire open and short tail defects, low stitch pull readings, and even nonstick on lead.

From the view of capillary design, possible solutions to these problems are optimization of the tip diameter, face angle, and outer radius, and surface finishing of the capillaries. However, the tip diameter is limited by the bond pad pitch of the devices. For example, for a bond pad pitch of 50 μm, the maximum tip diameter allowed is 63 μm. Compared to the standard capillary design, a smaller face angle (8° compared to 11°) improves stitch bondability, but this can also lower stitch pull readings. A smaller outer radius (5 μm compared to 8 μm) also improves stitch bondability, but this can cause heel cracking [113]. The optimization of the capillary design in the chamfer diameter, chamfer angle, and face angle can result

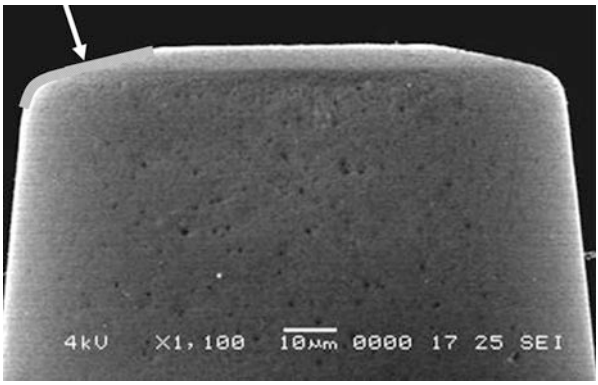

Fig. 2.14 Modified capillary design (the modified portion is shown by the *curved line*) [113]

in bonding being carried out with lower ultrasonic power and lower bonding force, which results in reduced Al splash and higher shear strength. For improved capillary design, considerations such as surface morphology, physical dimensions, and bonding process window need to be taken into account in engineering evaluations [114]. In order to ensure a long capillary lifetime, the choice of capillary material and its resistance to acoustic impedance are the parameters required to reduce the ultrasonic power requirement [45].

Second bond formation in Cu wire bonding requires the use of granular surface tools to minimize wire slippage during bonding and improve gripping between the wire and the capillary [113, 115, 116]. However, matte or granular finishes have the issue of buildup at the capillary, which reduces the capillary lifetime. The granular capillaries used in Cu wire bonding wear out quickly compared to the polished capillaries used in Au wire bonding. Teck et al. [107] studied the capillary touchdown limit for 47 µm bond pad pitch with 20 µm wire size. It was found that at 200k touchdowns, the capillary started wearing out. At 300k touchdowns, the buildup at the capillary wall resulted in stoppages due to short tail lengths. Therefore, it was recommended that the capillary life of the Cu wire should be controlled at the maximum number of 300k touchdowns to avoid stoppages.

Polished chamfers are used in the second bonds when reduced tip diameters are used and also where the surface bondability is good. Goh et al. [113, 116, 117] developed a capillary design with an enhanced capillary tip surface texture, a larger inner chamfer, a larger chamfer diameter, and a smaller chamfer angle for improved bondability (Fig. 2.14). The modified design led to smaller sized ball bonds, resulting in higher reliability under HTS tests.

Research has shown that the chamfer angle, chamfer diameter, and inside chamfer affect ball deformation [113, 116, 117]. Optimization of these dimensions can improve ball bondability. For example, compared to a standard design, an optimized capillary design has a smaller chamfer angle, a larger inner chamfer, and a larger chamfer diameter, which results in a smaller bonded ball size by limiting the amount of wire material inside the capillary during impact and restricting the softened wire material being squeezed out during wire bonding. About 40 % of the FAB can be contained within the inner chamfer. The new capillary design has been shown to improve ball bondability and small ball size control for ultrafine-pitch

wire bonding [116]. The continuous shrinking of IC chips with closer pad-to-pad pitches has resulted in an increase in demand for special wire bonding capillaries for ultrafine-pitch applications. As capillary tips become smaller, there is a need to redesign the external profiles of capillaries to provide consistent ultrasonic energy transfer during wire bonding [118].

In thermosonic bonding, the capillary vibration amplitude helps determine the reliability of the formed bonds. The maximum ultrasonic vibration should occur at or near the capillary tip for optimal bonding performance. The vibrational behavior of the capillary transmits the ultrasonic energy from the transducer to the interface of the bonding media. Depending on the ball size requirement and the bond power and force settings used, the displacement of the capillary tip during bonding can vary from 0.56 to 3 μm. Higher displacement results in a larger bonded ball size. Depending on the capillary design, the node point can be positioned nearer or farther away from the capillary tip. By moving the node point away from the capillary tip, larger tip displacement can be achieved. Although the vibration amplitude of a capillary depends on the location of the node point, the overall capillary length also affects the vibration behavior. Other factors, such as the internal taper angle, tip diameter, and bottleneck height, also affect the vibration characteristics of a capillary. These dimensions change the displacement amplitude at the capillary tip, which is directly responsible for the bond quality of ball and stitch bonds.

Capillaries with bottlenecks are used for ultrafine-pitch bonding, as their slim profile near the tip can prevent contact with adjacent wires. For wire bonding of low-k ultrafine-pitch devices, relatively low USG power is needed to prevent pad damage. Optimization of the external profile of a capillary can make the capillary transfer ultrasonic vibrations in the preferred direction with low USG power. The ultrasonic vibration displacements of the capillaries were measured by Goh et al. [117] using a laser interferometer. The measurements showed that the ratio of the vibration displacement at the capillary tip to that at the transducer point of a capillary with a small radius transition between the main taper angle and the bottleneck angle was 37 % higher than that of a capillary with a sharp transition, in terms of ball shear (0.102 vs. 0.099 N) and stitch pull strength (0.061 vs. 0.059 N). To solve the ball lift (non-sticking) problem for wire bonding of low-k ultrafine-pitch devices, optimization of the capillary internal profile was attempted [117]. Compared to a standard design, a capillary with a larger inner chamfer, a smaller chamfer angle, and a larger chamfer diameter increased the percentage of the intermetallic compound in the bond interface and improved bondability. Ball lift failure and metal pad peeling were not observed after an aging test. Zhong et al. [118] investigated the effect of ultrasonic vibration on the capillaries with varying zirconia composition and found that the capillaries with the lowest zirconia compositions are most suitable for fine-pitch applications. If the critical capillary dimensions are not optimized, failure can occur. Several failure modes could arise because of incorrect design, selection, and usage of the tool (capillary) or tool wear-out. Table 2.4 provides details about the types of failure modes of wire bonds and their potential root causes.

Table 2.4 Failure mechanisms and potential root causes of wire bond failures

Mechanism	Potential root cause
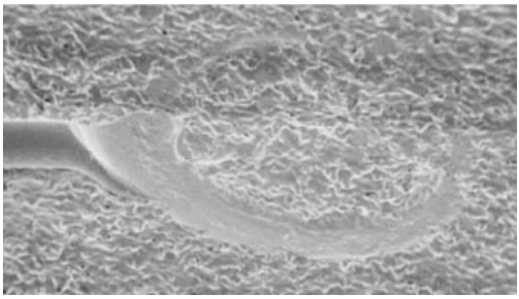	Caused by small capillary diameter or worn-out capillary.

Fig. 2.15 Weak, chopped-off, or cut bond [112]

	Caused by poor wetting due to poor plating or contamination. Other causes could be improper bonding conditions or capillary dimensions that are too small.

Fig. 2.16 Non-sticking second bonds [112]

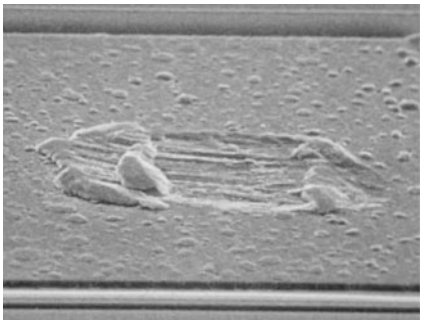

Fig. 2.17 Ball bond not sticking to the pad [112]

(continued)

Table 2.4 (continued)

Mechanism	Potential root cause
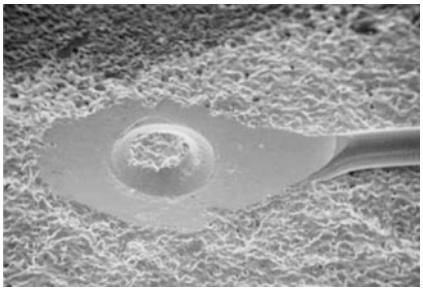	Caused by a shallow face angle of the capillary; smaller outside capillary radius compared to wire size, excessive bond force, high-frequency setting, or improper clamping of the substrate.

Fig. 2.18 Weak transition from the wedge bond to the wire [112]

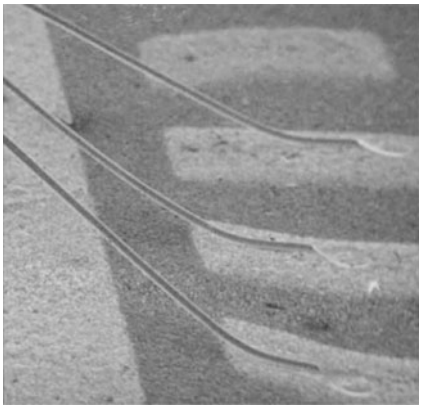	Caused by excessive wire length or a wire diameter that is too small for the loop length.

Fig. 2.19 Wavy or sagging wire [112]

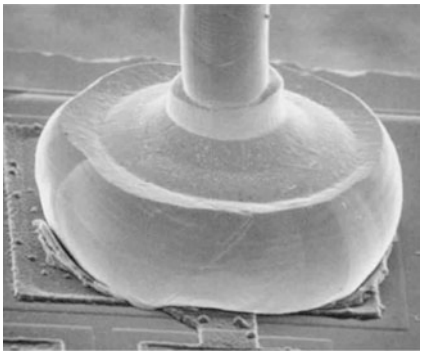	Caused by a wire or a free air ball size that is too large.

Fig. 2.20 Larger ball bond than desired [112]

(continued)

Table 2.4 (continued)

Mechanism	Potential root cause
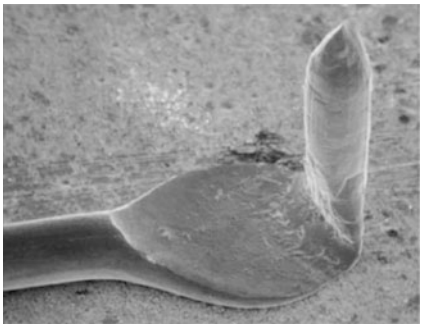	Caused by shallow angle causing a strong tail bond and excessive wire length.
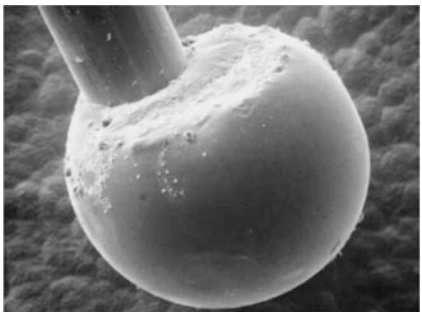	Caused by poor bonding surface, contamination, and excessive wire hardness.
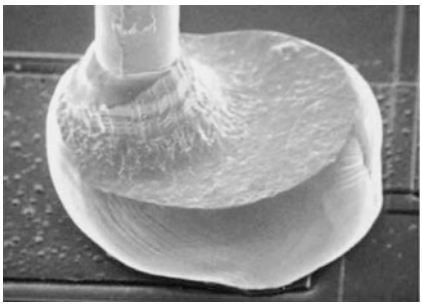	Caused by poor bonding surface, contamination, and excessive wire hardness.

Fig. 2.21 Tailing problem associated with thermocompression bonding [112]

Fig. 2.22 Off-center FAB [112]

Fig. 2.23 Golf club bond [112]

(continued)

Table 2.4 (continued)

Mechanism	Potential root cause
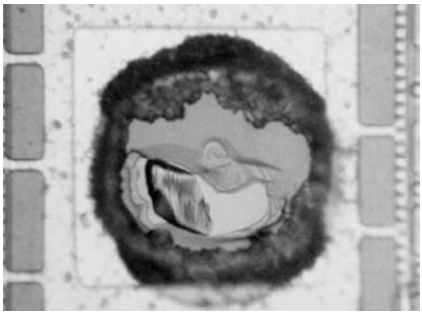	Caused by excessive bond energy, poor adhesion of the metal, brittleness of the bond pad, or improper clamping of the substrate.
Fig. 2.24 Pad cratering [112]	
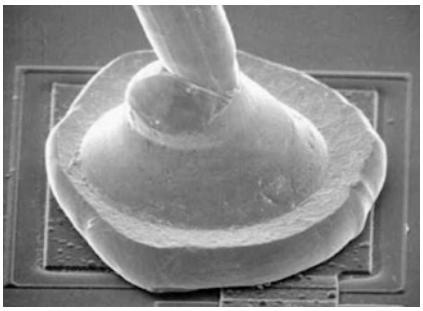	Caused by insufficient force during bonding, improper bond location, and/or an FAB that is too small.
Fig. 2.25 Necking above the ball bond [112]	

2.8 Summary

In this chapter, the details of the bonding process, including the properties and types of bonding wire, were discussed. During thermosonic bonding, heat softens the bonding wire and the board metallization, and bonding is carried out by adjusting the bonding force and ultrasonic energy. The bonding process must be optimized to minimize defects and form a reliable joint.

The optimum ultrasonic power should be determined to achieve good bond quality. Insufficient power has been shown to result in under-formed bonds and tail lifts. However, excessive power can result in a squashed appearance, cracks, and cratering damage to the underlying structure on the semiconductor die. Ball deformation and ball shear force increase with an increase in USG current. The optimum USG current should be determined to achieve uniform ball bonds.

Other parameters for bonding process optimization include EFO current and firing time, cover gas flow rate, bonding force, and bonding temperature. EFO

current is supplied to form FABs. The micro-hardness of bonded Cu balls is related to the EFO parameters with softer FABs obtained by higher EFO current.

Comparisons of bare Cu and PdCu wires have shown that at a higher EFO current, FABs with bare Cu wire have higher hardness than PdCu wires because they have smaller grains. For PdCu wire, changing the EFO current varies the hardness because of the different distributions of the PdCu alloy in the FAB.

The effect of gas flow rate on FAB formation was also discussed. A slow flow rate causes an asymmetric shape of the FAB, and, thus, is unacceptable from a reliability standpoint. Therefore, based on the wire diameter and type of EFO current, the gas flow rate should be optimized.

The bond force is the downward force exerted by the bonding head during bonding. A high bonding force is not desirable since it can damage the pad or cause pad cratering. On the other hand, a low bonding force is not desirable either, since it leads to the NSOP condition. Bonding temperature softens the wire and thus improves the deformability of the wire and the FAB, and also increases the diffusion at the FAB–bond pad interface. However, high temperatures can result in rigidity loss for board materials, causing bonds to lift.

Bond process optimization is essential for Cu wire bonding, since it has a narrower process window than the Au wire bonding. Researchers have adopted statistical techniques such as Six Sigma DMAIC methodology and statistical DOE for process optimization of Cu wire bonding. Along with the bonding process, the bonding tool could also damage the bond. Several damage mechanisms that can occur due to improper bonding tool usage or dimensions were discussed. To achieve a quality joint, the surface must be contamination free, the tool must be maintained, the process parameters must be optimized, and there must be an optimal bonding environment.

http://www.springer.com/978-1-4614-5760-2

Copper Wire Bonding

Chauhan, P.S.; Choubey, A.; Zhong, Z.; Pecht, M.G.

2014, XXVI, 235 p. 104 illus., 20 illus. in color.,
Hardcover
ISBN: 978-1-4614-5760-2